

First joint oscillation analysis of Super-Kamiokande atmospheric and T2K accelerator neutrino data

K. Abe,^{1,48} S. Abe,¹ C. Bronner,¹ Y. Hayato,^{1,48} K. Hiraide,^{1,48} K. Hosokawa,¹ K. Ieki,^{1,48} M. Ikeda,^{1,48} J. Kameda,^{1,48} Y. Kanemura,¹ R. Kaneshima,¹ Y. Kashiwagi,¹ Y. Kataoka,^{1,48} S. Miki,¹ S. Mine,^{1,6} M. Miura,^{1,48} S. Moriyama,^{1,48} M. Nakahata,^{1,48} Y. Nakano,¹ S. Nakayama,^{1,48} Y. Noguchi,¹ K. Sato,¹ H. Sekiya,^{1,48} H. Shiba,¹ K. Shimizu,¹ M. Shiozawa,^{1,48} Y. Sonoda,¹ Y. Suzuki,¹ A. Takeda,^{1,48} Y. Takemoto,^{1,48} H. Tanaka,^{1,48} T. Yano,¹ S. Han,² T. Kajita,^{2,48,22} K. Okumura,^{2,48} T. Tashiro,² T. Tomiya,² X. Wang,² S. Yoshida,² P. Fernandez,³ L. Labarga,³ N. Ospina,³ B. Zaldivar,³ B. W. Pointon,^{5,51} E. Kearns,^{4,48} J. Mirabito,⁴ J. L. Raaf,⁴ L. Wan,⁴ T. Wester,⁴ J. Bian,⁶ N. J. Griskevich,⁶ M. B. Smy,^{6,48} H. W. Sobel,^{6,48} V. Takhistov,^{6,24} A. Yankelevich,⁶ J. Hill,⁷ M. C. Jang,⁸ S. H. Lee,⁸ D. H. Moon,⁸ R. G. Park,⁸ B. Bodur,⁹ K. Scholberg,^{9,48} C. W. Walter,^{9,48} A. Beauchêne,¹⁰ O. Drapier,¹⁰ A. Giampaolo,¹⁰ Th. A. Mueller,¹⁰ A. D. Santos,¹⁰ P. Paganini,¹⁰ B. Quilain,¹⁰ R. Rogly,¹⁰ T. Nakamura,¹¹ J. S. Jang,¹² L. N. Machado,¹³ J. G. Learned,¹⁴ K. Choi,¹⁵ N. Iovine,¹⁵ S. Cao,¹⁶ L. H. V. Anthony,¹⁷ D. Martin,¹⁷ N. W. Prouse,¹⁷ M. Scott,¹⁷ Y. Uchida,¹⁷ V. Berardi,¹⁸ N. F. Calabria,¹⁸ M. G. Catanesi,¹⁸ E. Radicioni,¹⁸ A. Langella,¹⁹ G. De Rosa,¹⁹ G. Collazuol,²⁰ M. Feltre,²⁰ F. Iacob,²⁰ M. Mattiuzzi,²⁰ L. Ludovici,²¹ M. Gonin,²² L. Périssé,²² G. Pronost,²² C. Fujisawa,²³ S. Horiuchi,²³ M. Kobayashi,²³ Y.M. Liu,²³ Y. Maekawa,²³ Y. Nishimura,²³ R. Okazaki,²³ R. Akutsu,²⁴ M. Friend,²⁴ T. Hasegawa,²⁴ T. Ishida,²⁴ T. Kobayashi,²⁴ M. Jakkapu,²⁴ T. Matsubara,²⁴ T. Nakadaira,²⁴ K. Nakamura,^{24,48} Y. Oyama,²⁴ A. Portocarrero Yrey,²⁴ K. Sakashita,²⁴ T. Sekiguchi,²⁴ T. Tsukamoto,²⁴ N. Bhuiyan,²⁵ G. T. Burton,²⁵ F. Di Lodovico,²⁵ J. Gao,²⁵ A. Goldsack,²⁵ T. Katori,²⁵ J. Migenda,²⁵ R. M. Ramsden,²⁵ Z. Xie,²⁵ S. Zsoldos,^{25,48} A. T. Suzuki,²⁶ Y. Takagi,²⁶ Y. Takeuchi,^{26,48} H. Zhong,²⁶ J. Feng,²⁷ L. Feng,²⁷ J. R. Hu,²⁷ Z. Hu,²⁷ M. Kawaue,²⁷ T. Kikawa,²⁷ M. Mori,²⁷ T. Nakaya,^{27,48} R. A. Wendell,^{27,48} K. Yasutome,²⁷ S. J. Jenkins,²⁸ N. McCauley,²⁸ P. Mehta,²⁸ A. Tarrant,²⁸ M. J. Wilking,²⁹ Y. Fukuda,³⁰ Y. Itow,^{31,32} H. Menjo,³¹ K. Ninomiya,³¹ Y. Yoshioka,³¹ J. Lagoda,³³ M. Mandal,³³ P. Mijakowski,³³ Y. S. Prabhu,³³ J. Zalipska,³³ M. Jia,³⁴ J. Jiang,³⁴ W. Shi,³⁴ C. Yanagisawa,^{34,*} M. Harada,³⁵ Y. Hino,³⁵ H. Ishino,³⁵ Y. Koshio,^{35,48} F. Nakanishi,³⁵ S. Sakai,³⁵ T. Tada,³⁵ T. Tano,³⁵ T. Ishizuka,³⁶ G. Barr,³⁷ D. Barrow,³⁷ L. Cook,^{37,48} S. Samani,³⁷ D. Wark,^{37,43} A. Holin,³⁸ F. Nova,³⁸ S. Jung,³⁹ B. S. Yang,³⁹ J. Y. Yang,³⁹ J. Yoo,³⁹ J. E. P. Fannon,⁴⁰ L. Kneale,⁴⁰ M. Malek,⁴⁰ J. M. McElwee,⁴⁰ M. D. Thiesse,⁴⁰ L. F. Thompson,⁴⁰ S. T. Wilson,⁴⁰ H. Okazawa,⁴¹ S. M. Lakshmi,⁴² S. B. Kim,⁴⁴ E. Kwon,⁴⁴ J. W. Seo,⁴⁴ I. Yu,⁴⁴ A. K. Ichikawa,⁴⁵ K. D. Nakamura,⁴⁵ S. Tairafune,⁴⁵ K. Nishijima,⁴⁶ A. Eguchi,⁴⁷ K. Nakagiri,⁴⁷ Y. Nakajima,^{47,48} S. Shima,⁴⁷ N. Taniuchi,⁴⁷ E. Watanabe,⁴⁷ M. Yokoyama,^{47,48} P. de Perio,⁴⁸ S. Fujita,⁴⁸ C. Jesús-Valls,⁴⁸ K. Martens,⁴⁸ K. M. Tsui,⁴⁸ M. R. Vagins,^{48,6} J. Xia,⁴⁸ S. Izumiyama,⁴⁹ M. Kuze,⁴⁹ R. Matsumoto,⁴⁹ K. Terada,⁴⁹ R. Asaka,⁵⁰ M. Ishitsuka,⁵⁰ H. Ito,⁵⁰ Y. Ommura,⁵⁰ N. Shigeta,⁵⁰ M. Shinoki,⁵⁰ K. Yamauchi,⁵⁰ T. Yoshida,⁵⁰ R. Gaur,⁵¹ V. Gousy-Leblanc,^{51,†} M. Hartz,⁵¹ A. Konaka,⁵¹ X. Li,⁵¹ S. Chen,⁵² B. D. Xu,⁵² Y. Wu,⁵² A.Q. Zhang,⁵² B. Zhang,⁵² M. Posiadala-Zezula,⁵³ S. B. Boyd,⁵⁴ R. Edwards,⁵⁴ D. Hadley,⁵⁴ M. Nicholson,⁵⁴ M. O'Flaherty,⁵⁴ B. Richards,⁵⁴ A. Ali,^{55,51} B. Jamieson,⁵⁵ S. Amanai,⁵⁶ Ll. Martí,⁵⁶ A. Minamino,⁵⁶ R. Shibayama,⁵⁶ R. Shimamura,⁵⁶ and S. Suzuki⁵⁶

(The Super-Kamiokande Collaboration)

K. Abe,¹ S. Abe,¹ N. Akhlaq,⁸³ R. Akutsu,²⁴ H. Alarackia-Charles,⁷⁵ A. Ali,^{55,51} Y.I. Alj Hakim,¹⁷ S. Alonso Monsalve,⁶³ C. Andreopoulos,²⁸ L. Anthony,¹⁷ M. Antonova,⁷² S. Aoki,²⁶ K.A. Apte,¹⁷ T. Arai,⁴⁷ T. Arihara,⁹¹ S. Arimoto,²⁷ Y. Asada,⁵⁶ Y. Ashida,²⁷ E.T. Atkin,¹⁷ N. Babu,⁷⁷ M. Barbi,⁸⁴ G.J. Barker,⁵⁴ G. Barr,³⁷ D. Barrow,³⁷ P. Bates,²⁸ M. Batkiewicz-Kwasniak,⁶⁸ V. Berardi,¹⁸ L. Berns,⁴⁵ S. Bhadra,⁹⁵ A. Blanchet,⁶⁶ A. Blondel,^{89,66} S. Bolognesi,⁵⁹ S. Bordoni,⁶⁶ S.B. Boyd,⁵⁴ A. Bravar,⁶⁶ C. Bronner,¹ A. Bubak,⁴² M. Buizza Avanzini,¹⁰ J.A. Caballero,⁸⁸ N.F. Calabria,¹⁸ S. Cao,¹⁶ D. Carabadjac,^{10,‡} A.J. Carter,⁸⁶ S.L. Cartwright,⁴⁰ M.P. Casado,⁷⁰ M.G. Catanesi,¹⁸ A. Cervera,⁷² J. Chakrani,⁷⁶ A. Chalumeau,⁸⁹ D. Cherdack,⁶⁹ P.S. Chong,⁸¹ A. Chvirova,⁷³ M. Cicerchia,²⁰ J. Coleman,²⁸ G. Collazuol,²⁰ L. Cook,^{37,48} F. Cormier,⁵¹ A. Cudd,⁶⁰ D. D'ago,²⁰ C. Dalmazzone,⁸⁹ T. Daret,⁵⁹ P. Dasgupta,⁶² C. Davis,⁸¹ Yu.I. Davydov,⁷⁸ A. De Roeck,⁶⁵ G. De Rosa,¹⁹ T. Dealtry,⁷⁵ C.C. Delogu,²⁰ C. Densham,⁴³ A. Dergacheva,⁷³ R. Dharmapal,⁹⁴ F. Di Lodovico,²⁵ G. Diaz Lopez,⁸⁹ S. Dolan,⁶⁵ D. Douqa,⁶⁶ T.A. Doyle,³⁴ O. Drapier,¹⁰ K.E. Duffy,³⁷ J. Dumarchez,⁸⁹ P. Dunne,¹⁷ K. Dygnarowicz,⁹³ A. Eguchi,⁴⁷ J. Elias,⁸⁵ S. Emery-Schrenk,⁵⁹ G. Erofeev,⁷³ A. Ershova,¹⁰ G. Eurin,⁵⁹ D. Fedorova,⁷³ S. Fedotov,⁷³ M. Feltre,²⁰ L. Feng,²⁷ D. Ferlewicz,⁴⁷ A.J. Finch,⁷⁵ G.A. Fiorentini Aguirre,⁹⁵ G. Fiorillo,¹⁹ M.D. Fitton,⁴³ J.M. Franco Patiño,⁸⁸ M. Friend,^{24,§} Y. Fujii,^{24,§} Y. Fukuda,³⁰ Y. Furui,⁹¹ L. Giannessi,⁶⁶ C. Giganti,⁸⁹ V. Glagolev,⁷⁸ M. Gonin,²² J. González Rosa,⁸⁸ E.A.G. Goodman,¹³ A. Gorin,⁷³ K. Gorshanov,⁷³ M. Grassi,²⁰ M. Guigue,⁸⁹ D.R. Hadley,⁵⁴

J.T. Haigh,⁵⁴ S. Han,² D.A. Harris,⁹⁵ M. Hartz,^{51, 48} T. Hasegawa,^{24, §} S. Hassani,⁵⁹ N.C. Hastings,²⁴ Y. Hayato,^{1, 48}
 I. Heitkamp,⁴⁵ D. Henaff,²⁰ Y. Hino,³⁵ M. Hogan,⁶¹ J. Holeczek,⁴² A. Holin,⁴³ T. Holvey,³⁷ N.T. Hong Van,⁷⁴
 T. Honjo,⁸⁰ K. Hosokawa,¹ J. Hu,²⁷ A.K. Ichikawa,⁴⁵ K. Ieki,¹ M. Ikeda,¹ T. Ishida,^{24, §} M. Ishitsuka,⁵⁰ A. Izmaylov,⁷³
 M. Jakkapu,²⁴ B. Jamieson,⁵⁵ S.J. Jenkins,²⁸ C. Jesús-Valls,⁴⁸ M. Jia,³⁴ J.J. Jiang,³⁴ J.Y. Ji,³⁴ P. Jonsson,¹⁷
 S. Joshi,⁵⁹ C.K. Jung,^{34, ¶} M. Kabirnezhad,¹⁷ A.C. Kabout,^{86, 43} T. Kajita,^{2, ¶} H. Kakuno,⁹¹ J. Kameda,¹
 S. Karpova,⁶⁶ S.P. Kasetti,⁷⁷ V.S. Kasturi,⁶⁶ Y. Kataoka,¹ T. Katori,²⁵ Y. Kawamura,⁸⁰ M. Kawaue,²⁷ E. Kearns,^{4, ¶}
 M. Khabibullin,⁷³ A. Khotjantsev,⁷³ T. Kikawa,²⁷ S. King,²⁵ V. Kiseeva,⁷⁸ J. Kisiel,⁴² L. Kneale,⁴⁰ H. Kobayashi,⁴⁷
 T. Kobayashi,^{24, §} L. Koch,⁷¹ S. Kodama,⁴⁷ M. Kolupanova,⁷³ A. Konaka,⁵¹ L.L. Kormos,⁷⁵ Y. Koshio,^{35, ¶}
 T. Koto,⁹¹ K. Kowalik,³³ Y. Kudenko,^{73, ¶} Y. Kudo,⁵⁶ S. Kuribayashi,²⁷ R. Kurjata,⁹³ V. Kurochka,⁷³ T. Kutter,⁷⁷
 M. Kuze,⁴⁹ M. La Commara,¹⁹ L. Labarga,³ M. Lachat,⁸⁵ K. Lachner,⁵⁴ J. Lagoda,³³ S.M. Lakshmi,⁴² M. Lamers
 James,^{75, 43} A. Langella,¹⁹ J.-F. Laporte,⁵⁹ D. Last,⁸⁵ N. Latham,⁵⁴ M. Laveder,²⁰ L. Lavitola,¹⁹ M. Lawe,⁷⁵ Y. Lee,²⁷
 D. Leon Silverio,⁹⁰ S. Levorato,²⁰ S. Lewis,²⁵ C. Lin,¹⁷ R.P. Litchfield,¹³ S.L. Liu,³⁴ W. Li,³⁷ A. Longhin,²⁰
 K.R. Long,^{17, 43} A. Lopez Moreno,²⁵ L. Ludovici,²¹ X. Lu,⁵⁴ T. Lux,⁷⁰ L.N. Machado,¹³ L. Magaletti,¹⁸ K. Mahn,⁷⁹
 K.K. Mahtani,³⁴ M. Malek,⁴⁰ M. Mandal,³³ S. Manly,⁸⁵ A.D. Marino,⁶⁰ L. Marti-Magro,⁵⁶ D.G.R. Martin,¹⁷
 M. Martini,^{89, **} J.F. Martin,⁹² T. Maruyama,^{24, §} T. Matsubara,²⁴ R. Matsumoto,⁴⁹ V. Matveev,⁷³ C. Mauger,⁸¹
 K. Mavrokoridis,²⁸ E. Mazzucato,⁵⁹ N. McCauley,²⁸ K.S. McFarland,⁸⁵ C. McGrew,³⁴ J. McKean,¹⁷ A. Mefodiev,⁷³
 G.D. Megias,⁸⁸ P. Mehta,²⁸ L. Mellet,⁷⁹ C. Metelko,²⁸ M. Mezzetto,²⁰ S. Miki,¹ E. Miller,²⁵ A. Minamino,⁵⁶
 O. Mineev,⁷³ S. Mine,^{1, 6} M. Miura,^{1, ¶} L. Molina Bueno,⁷² S. Moriyama,^{1, ¶} S. Moriyama,⁵⁶ P. Morrison,¹³
 Th.A. Mueller,¹⁰ D. Munford,⁶⁹ A. Muñoz,^{10, 22} L. Munteanu,⁶⁵ K. Nagai,⁵⁶ Y. Nagai,⁶² T. Nakadaira,^{24, §}
 K. Nakagiri,⁴⁷ M. Nakahata,^{1, 48} Y. Nakajima,⁴⁷ A. Nakamura,³⁵ K. Nakamura,^{48, 24, §} K.D. Nakamura,⁴⁵ Y. Nakano,¹
 S. Nakayama,^{1, 48} T. Nakaya,^{27, 48} K. Nakayoshi,^{24, §} C.E.R. Naseby,¹⁷ T.V. Ngoc,²⁷ D.T. Nguyen,⁶⁴ V.Q. Nguyen,¹⁰
 K. Niewczas,⁶⁷ S. Nishimori,²⁴ Y. Nishimura,²³ Y. Noguchi,¹ T. Nosek,³³ F. Nova,⁴³ P. Novella,⁷² J.C. Nugent,⁴⁵
 H.M. O’Keeffe,⁷⁵ L. O’Sullivan,⁷¹ T. Odagawa,²⁷ R. Okazaki,²³ W. Okinaga,⁴⁷ K. Okumura,^{2, 48} T. Okusawa,⁸⁰
 N. Onda,²⁷ N. Ospina,³ L. Osu,¹⁰ Y. Oyama,^{24, §} V. Palladino,¹⁹ V. Paolone,⁸² M. Pari,²⁰ J. Parlone,²⁸
 J. Pasternak,¹⁷ D. Payne,²⁸ G.C. Penn,²⁸ D. Pershey,⁹ M. Pfaff,¹⁷ L. Pickering,⁴³ G. Pintaudi,⁵⁶ C. Pistillo,⁵⁷
 B. Popov,^{89, ††} A.J. Portocarrero Yrey,²⁴ K. Porwit,⁴² M. Posiadala-Zezula,⁵³ Y.S. Prabhu,³³ H. Prasad,⁹⁴
 F. Pupilli,²⁰ B. Quilain,¹⁰ P.T. Quyen,^{16, ††} T. Radermacher,⁸⁷ E. Radicioni,¹⁸ B. Radics,⁹⁵ M.A. Ramirez,⁸¹
 P.N. Ratoff,⁷⁵ M. Reh,⁶⁰ C. Riccio,³⁴ E. Rondio,³³ S. Roth,⁸⁷ N. Roy,⁹⁵ A. Rubbia,⁶³ L. Russo,⁸⁹ A. Rychter,⁹³
 W. Saenz,⁸⁹ K. Sakashita,^{24, §} F. Sánchez,⁶⁶ Y. Sato,⁵⁰ T. Scheffe,⁷⁷ C.M. Schloesser,⁶⁶ K. Scholberg,^{9, ¶} M. Scott,¹⁷
 Y. Seiya,^{80, ¶¶} T. Sekiguchi,^{24, §} H. Sekiya,^{1, 48, ¶} D. Sgalaberna,⁶³ A. Shaikhiev,⁷³ M. Shiozawa,^{1, 48} Y. Shiraishi,³⁵
 A. Shvartsman,⁷³ N. Skrobova,⁷³ K. Skwarczynski,⁸⁶ D. Smyczek,⁸⁷ M. Smy,⁶ J.T. Sobczyk,⁹⁴ H. Sobel,^{6, 48}
 F.J.P. Soler,¹³ A.J. Speers,⁷⁵ R. Spina,¹⁸ Y. Stroke,⁷³ I.A. Suslov,⁷⁸ S. Suvorov,^{73, 89} A. Suzuki,²⁶ S.Y. Suzuki,^{24, §}
 Y. Suzuki,⁴⁸ M. Tada,^{24, §} S. Tairafune,⁴⁵ A. Takeda,¹ Y. Takeuchi,^{26, 48} K. Takifuji,⁴⁵ H.K. Tanaka,^{1, ¶}
 H. Tanigawa,²⁴ A. Teklu,³⁴ V.V. Tereshchenko,⁷⁸ N. Thamm,⁸⁷ L.F. Thompson,⁴⁰ W. Toki,⁶¹ C. Touramanis,²⁸
 T. Tsukamoto,^{24, §} M. Tzanov,⁷⁷ Y. Uchida,¹⁷ M. Vagins,^{48, 6} D. Vargas,⁷⁰ M. Varghese,⁷⁰ G. Vasseur,⁵⁹ E. Villa,^{65, 66}
 W.G.S. Vinning,⁵⁴ U. Virginet,⁸⁹ T. Vladisavljevic,⁴³ T. Wachala,⁶⁸ D. Wakabayashi,⁴⁵ H.T. Wallace,⁴⁰
 J.G. Walsh,⁷⁹ Y. Wang,³⁴ L. Wan,⁴ D. Wark,^{43, 37} M.O. Wascko,^{37, 43} A. Weber,⁷¹ R. Wendell,²⁷ M.J. Wilking,²⁹
 C. Wilkinson,⁷⁶ J.R. Wilson,²⁵ K. Wood,⁷⁶ C. Wret,³⁷ J. Xia,⁴⁸ Y.-h. Xu,⁷⁵ K. Yamamoto,^{80, ¶¶} T. Yamamoto,⁸⁰
 C. Yanagisawa,^{34, *} G. Yang,³⁴ T. Yano,¹ K. Yasutome,²⁷ N. Yershov,⁷³ U. Yevarouskaya,³⁴ M. Yokoyama,^{47, ¶}
 Y. Yoshimoto,⁴⁷ N. Yoshimura,²⁷ M. Yu,⁹⁵ R. Zaki,⁹⁵ A. Zalewska,⁶⁸ J. Zalipska,³³ K. Zarembo,⁹³ G. Zarnecki,⁶⁸
 J. Zhang,^{51, 58} X.Y. Zhao,⁶³ H. Zhong,²⁶ T. Zhu,¹⁷ M. Ziembicki,⁹³ E.D. Zimmerman,⁶⁰ M. Zito,⁸⁹ and S. Zsoldos²⁵

(The T2K Collaboration)

¹University of Tokyo, Institute for Cosmic Ray Research, Kamioka Observatory, Kamioka, Japan

²University of Tokyo, Institute for Cosmic Ray Research, Research Center for Cosmic Neutrinos, Kashiwa, Japan

³University Autonoma Madrid, Department of Theoretical Physics, Madrid, Spain

⁴Boston University, Department of Physics, Boston, Massachusetts, U.S.A.

⁵British Columbia Institute of Technology, Department of Physics, Burnaby, British Columbia, Canada

⁶University of California, Irvine, Department of Physics and Astronomy, Irvine, California, U.S.A.

⁷California State University, Department of Physics, Dominguez Hills, Carson, California, U.S.A

⁸Chonnam National University, Institute for Universe and Elementary Particles, Gwangju, Korea

⁹Duke University, Department of Physics, Durham, North Carolina, U.S.A.

¹⁰Ecole Polytechnique, IN2P3-CNRS, Laboratoire Leprince-Ringuet, Palaiseau, France

¹¹Gifu University, Department of Physics, Gifu, Japan

¹²Gwangju Institute of Science and Technology, GIST College, Gwangju, Korea

¹³University of Glasgow, School of Physics and Astronomy, Glasgow, United Kingdom

- ¹⁴University of Hawaii, Department of Physics and Astronomy, Honolulu, Hawaii, U.S.A.
- ¹⁵Institute for Basic Science (IBS), Center for Underground Physics, Daejeon, Korea
- ¹⁶Institute For Interdisciplinary Research in Science and Education (IFIRSE), ICISE, Quy Nhon, Vietnam
- ¹⁷Imperial College London, Department of Physics, London, United Kingdom
- ¹⁸INFN Sezione di Bari and Università e Politecnico di Bari, Dipartimento Interuniversitario di Fisica, Bari, Italy
- ¹⁹INFN Sezione di Napoli and Università di Napoli, Dipartimento di Fisica, Napoli, Italy
- ²⁰INFN Sezione di Padova and Università di Padova, Dipartimento di Fisica, Padova, Italy
- ²¹INFN Sezione di Roma and Università di Roma "La Sapienza", Roma, Italy
- ²²ILANCE, CNRS – University of Tokyo International Research Laboratory, Kashiwa, Chiba, Japan
- ²³Keio University, Department of Physics, Kanagawa, Japan
- ²⁴High Energy Accelerator Research Organization (KEK), Tsukuba, Ibaraki, Japan
- ²⁵King's College London, Department of Physics, Strand, London, United Kingdom
- ²⁶Kobe University, Kobe, Japan
- ²⁷Kyoto University, Department of Physics, Kyoto, Japan
- ²⁸University of Liverpool, Department of Physics, Liverpool, United Kingdom
- ²⁹University of Minnesota, School of Physics and Astronomy, Minneapolis, Minnesota, U.S.A.
- ³⁰Miyagi University of Education, Department of Physics, Sendai, Japan
- ³¹Nagoya University, Institute for Space-Earth Environmental Research, Nagoya, Aichi, Japan
- ³²Nagoya University, Kobayashi-Maskawa Institute for the Origin of Particles and the Universe, Nagoya, Aichi, Japan
- ³³National Centre for Nuclear Research, Warsaw, Poland
- ³⁴State University of New York at Stony Brook, Department of Physics and Astronomy, Stony Brook, New York, U.S.A.
- ³⁵Okayama University, Department of Physics, Okayama, Japan
- ³⁶Osaka Electro-Communication University, Media Communication Center, Neyagawa, Osaka, Japan
- ³⁷Oxford University, Department of Physics, Oxford, United Kingdom
- ³⁸Rutherford Appleton Laboratory, Harwell, Oxford, United Kingdom
- ³⁹Seoul National University, Department of Physics, Seoul, Korea
- ⁴⁰University of Sheffield, Department of Physics and Astronomy, Sheffield, United Kingdom
- ⁴¹Shizuoka University of Welfare, Department of Informatics in Social Welfare, Yaizu, Shizuoka, Japan
- ⁴²University of Silesia, Institute of Physics, Katowice, Poland
- ⁴³STFC, Rutherford Appleton Laboratory, Harwell Oxford, and Daresbury Laboratory, Warrington, United Kingdom
- ⁴⁴Sungkyunkwan University, Department of Physics, Suwon, Korea
- ⁴⁵Tohoku University, Faculty of Science, Department of Physics, Miyagi, Japan
- ⁴⁶Tokai University, Department of Physics, Hiratsuka, Kanagawa, Japan
- ⁴⁷University of Tokyo, Department of Physics, Tokyo, Japan
- ⁴⁸Kavli Institute for the Physics and Mathematics of the Universe (WPI), The University of Tokyo Institutes for Advanced Study, University of Tokyo, Kashiwa, Chiba, Japan
- ⁴⁹Tokyo Institute of Technology, Department of Physics, Tokyo, Japan
- ⁵⁰Tokyo University of Science, Faculty of Science and Technology, Department of Physics, Noda, Chiba, Japan
- ⁵¹TRIUMF, Vancouver, British Columbia, Canada
- ⁵²Tsinghua University, Department of Engineering Physics, Beijing, China
- ⁵³University of Warsaw, Faculty of Physics, Warsaw, Poland
- ⁵⁴University of Warwick, Department of Physics, Coventry, United Kingdom
- ⁵⁵University of Winnipeg, Department of Physics, Winnipeg, Manitoba, Canada
- ⁵⁶Yokohama National University, Department of Physics, Yokohama, Japan
- ⁵⁷University of Bern, Albert Einstein Center for Fundamental Physics, Laboratory for High Energy Physics (LHEP), Bern, Switzerland
- ⁵⁸University of British Columbia, Department of Physics and Astronomy, Vancouver, British Columbia, Canada
- ⁵⁹IRFU, CEA, Université Paris-Saclay, Gif-sur-Yvette, France
- ⁶⁰University of Colorado at Boulder, Department of Physics, Boulder, Colorado, U.S.A.
- ⁶¹Colorado State University, Department of Physics, Fort Collins, Colorado, U.S.A.
- ⁶²Eötvös Loránd University, Department of Atomic Physics, Budapest, Hungary
- ⁶³ETH Zurich, Institute for Particle Physics and Astrophysics, Zurich, Switzerland
- ⁶⁴Hanoi University of Science, Vietnam National University, Hanoi, Vietnam
- ⁶⁵CERN European Organization for Nuclear Research, Genève, Switzerland
- ⁶⁶University of Geneva, Section de Physique, DPNC, Geneva, Switzerland
- ⁶⁷Ghent University, Department of Physics and Astronomy, Gent, Belgium
- ⁶⁸H. Niewodniczanski Institute of Nuclear Physics PAN, Cracow, Poland
- ⁶⁹University of Houston, Department of Physics, Houston, Texas, U.S.A.
- ⁷⁰Institut de Física d'Altes Energies (IFAE) - The Barcelona Institute of Science and Technology, Campus UAB, Bellaterra (Barcelona) Spain
- ⁷¹Institut für Physik, Johannes Gutenberg-Universität Mainz, Staudingerweg 7, Mainz, Germany
- ⁷²IFIC (CSIC & University of Valencia), Valencia, Spain
- ⁷³Institute for Nuclear Research of the Russian Academy of Sciences, Moscow, Russia

⁷⁴*International Centre of Physics, Institute of Physics (IOP), Vietnam Academy of Science and Technology (VAST), 10 Dao Tan, Ba Dinh, Hanoi, Vietnam*

⁷⁵*Lancaster University, Physics Department, Lancaster, United Kingdom*

⁷⁶*Lawrence Berkeley National Laboratory, Berkeley, California, U.S.A.*

⁷⁷*Louisiana State University, Department of Physics and Astronomy, Baton Rouge, Louisiana, U.S.A.*

⁷⁸*Joint Institute for Nuclear Research, Dubna, Moscow Region, Russia*

⁷⁹*Michigan State University, Department of Physics and Astronomy, East Lansing, Michigan, U.S.A.*

⁸⁰*Osaka Metropolitan University, Department of Physics, Osaka, Japan*

⁸¹*University of Pennsylvania, Department of Physics and Astronomy, Philadelphia, Pennsylvania U.S.A.*

⁸²*University of Pittsburgh, Department of Physics and Astronomy, Pittsburgh, Pennsylvania, U.S.A.*

⁸³*Queen Mary University of London, School of Physics and Astronomy, London, United Kingdom*

⁸⁴*University of Regina, Department of Physics, Regina, Saskatchewan, Canada*

⁸⁵*University of Rochester, Department of Physics and Astronomy, Rochester, New York, U.S.A.*

⁸⁶*Royal Holloway University of London, Department of Physics, Egham, Surrey, United Kingdom*

⁸⁷*RWTH Aachen University, III. Physikalisches Institut, Aachen, Germany*

⁸⁸*Universidad de Sevilla, Departamento de Física Atómica, Molecular y Nuclear, Sevilla, Spain*

⁸⁹*Sorbonne Université, CNRS/IN2P3, Laboratoire de Physique Nucléaire et de Hautes Energies (LPNHE), Paris, France*

⁹⁰*South Dakota School of Mines and Technology, Rapid City, South Dakota, U.S.A.*

⁹¹*Tokyo Metropolitan University, Department of Physics, Tokyo, Japan*

⁹²*University of Toronto, Department of Physics, Toronto, Ontario, Canada*

⁹³*Warsaw University of Technology, Institute of Radioelectronics and Multimedia Technology, Warsaw, Poland*

⁹⁴*Wroclaw University, Faculty of Physics and Astronomy, Wroclaw, Poland*

⁹⁵*York University, Department of Physics and Astronomy, Toronto, Ontario, Canada*

(Dated: May 22, 2024)

The Super-Kamiokande and T2K collaborations present a joint measurement of neutrino oscillation parameters from their atmospheric and beam neutrino data. It uses a common interaction model for events overlapping in neutrino energy and correlated detector systematic uncertainties between the two datasets, which are found to be compatible. Using 3244.4 days of atmospheric data and a beam exposure of $19.7(16.3) \times 10^{20}$ protons on target in (anti)neutrino mode, the analysis finds a 1.9σ exclusion of CP-conservation (defined as $J_{\text{CP}} = 0$) and a preference for the normal mass ordering.

Introduction—Following the observation of neutrino oscillations [1], experiments now aim to fully characterize the three-flavor mixing paradigm described by the Pontecorvo–Maki–Nakagawa–Sakata matrix. Here, neutrino mixing is governed by three mixing angles (θ_{13} , θ_{23} , and θ_{12}), two mass splittings (Δm_{32}^2 and Δm_{21}^2), and one Charge Parity (CP) violating phase (δ_{CP}). While some oscillation parameters have been precisely measured [2], others remain relatively unconstrained. In particular, the CP-violating phase, the ordering of the neutrino mass states (MO), and the octant of θ_{23} have not been de-

termined experimentally. The Jarlskog invariant [3, 4], $J_{\text{CP}} = \sin \theta_{13} \cos^2 \theta_{13} \sin \theta_{12} \cos \theta_{12} \sin \theta_{23} \cos \theta_{23} \sin \delta_{\text{CP}}$, gives the magnitude of a potential CP violation.

Experimental setup—The Super-Kamiokande (SK) experiment [5] measures atmospheric neutrino oscillations using a large multi-purpose water Cherenkov detector located in the Kamioka mine in Gifu, Japan. The detector has a 32 kiloton inner detector optically separated from a 2 meter thick outer detector, which mainly serves as a veto region. Atmospheric neutrinos, produced by the interaction of cosmic rays with nuclei in the Earth’s atmosphere, include a mixture of neutrino flavor states, as well as a wide range of propagation baselines (15~13000 km) and neutrino energies (MeV~TeV).

The Tokai-to-Kamioka (T2K) long-baseline neutrino experiment [6] measures neutrino oscillations over a baseline of 295 km using a primarily muon (anti)neutrino beam produced by the neutrino facility at J-PARC, located in Ibaraki, Japan. SK is T2K’s far detector and measures neutrinos after oscillations 2.5° off of the beam axis. The beam neutrino flux and neutrino interaction cross sections are constrained by a suite of near detectors (T2K ND) situated 280 m downstream of the neutrino production target.

Motivation for a joint analysis—T2K’s off-axis neutrino beam provides a narrow energy spectrum peaked at 600 MeV and a known direction for beam-induced

* also at BMCC/CUNY, Science Department, New York, New York, U.S.A.

† also at University of Victoria, Department of Physics and Astronomy, PO Box 1700 STN CSC, Victoria, BC V8W 2Y2, Canada.

‡ also at Université Paris-Saclay

§ also at J-PARC, Tokai, Japan

¶ affiliated member at Kavli IPMU (WPI), the University of Tokyo, Japan

|| also at Moscow Institute of Physics and Technology (MIPT), Moscow region, Russia and National Research Nuclear University “MEPhI”, Moscow, Russia

** also at IPSA-DRII, France

†† also at JINR, Dubna, Russia

‡‡ also at the Graduate University of Science and Technology, Vietnam Academy of Science and Technology

¶¶ also at Nambu Yoichiro Institute of Theoretical and Experimental Physics (NITEP)

events at SK. This enables a precise determination of $\sin^2(2\theta_{23})$ and $|\Delta m_{32}^2|$ using the “disappearance” channels ($\bar{\nu}_\mu \rightarrow \bar{\nu}_\mu$), and some constraint on the CP-violating phase and the MO via the lower statistics “appearance” channels ($\bar{\nu}_\mu \rightarrow \bar{\nu}_e$). The beam composition can be changed from primarily neutrinos to primarily antineutrinos by switching the polarity of electromagnetic focusing horns, providing the ability to compare neutrino and antineutrino oscillations. T2K’s baseline probes the first oscillation maximum and matter effects have a limited impact. Nonetheless, there are notable parameter degeneracies between the MO and δ_{CP} [7]. Degeneracies between the lower and upper octants of θ_{23} also affect the measurements. SK’s atmospheric neutrino sample, on the other hand, provides a comparatively weak constraint on the atmospheric mixing parameters, due to limited information about the incoming neutrino direction, and a broader range of neutrino energies. However, upward-going neutrinos experience large matter effects, producing asymmetric oscillations between neutrinos and antineutrinos and providing sensitivity to both the octant of θ_{23} and the MO through the appearance channel at 2–10 GeV. This provides a means of breaking the MO– δ_{CP} degeneracy, complementing the MO sensitivity achieved at T2K through its lower energy $\bar{\nu}_e$ appearance events. Additionally, common systematic uncertainties at SK can be better constrained in a joint fit than in the individual experiments, due to the addition of the T2K ND constraints to the SK analysis and the large statistics atmospheric sample to the T2K analysis.

Analysis strategy—The analysis described here is based on previous analyses from the two experiments [8, 9], modified to produce a coherent joint analysis. Neutrino oscillation parameters are measured by comparing predictions for the rates and spectra of the atmospheric and beam neutrinos to observations performed at SK and making statistical inferences, following both frequentist and Bayesian approaches. The predictions are made using a model of the two experiments, covering neutrino fluxes, interactions, and detector response, with associated uncertainties. This model is built by unifying aspects of the two experiments’ analyses where appropriate, and using each individual experiment’s approach otherwise.

Due to the similarities in neutrino energy spectra and event selections, T2K and low energy atmospheric events are described by a common neutrino interaction model. The remaining SK atmospheric events correspond to neutrinos of higher energies, for which the constraint on interaction uncertainties coming from the lower energy neutrino measurements at the T2K ND is not always directly applicable. As a result, for these events, the same base interaction model is used for the initial simulation, but largely independent parameters are used for interaction systematic uncertainties. The neutrino flux models of the two experiments [8, 10, 11] are mostly independent, with the only common source of systematic uncertainty coming from hadron production in proton

collisions. Hadron production is tuned using different measurements in the two models: the SK atmospheric flux model uses atmospheric muon measurements [12, 13], whereas T2K’s flux model uses measurements by the NA61/SHINE experiment [14]. The resulting uncertainties on the flux prediction are therefore considered to be independent between the two models. The neutrino events of the two experiments are observed in the same detector, and the correlated effects of detector systematic uncertainties on SK and T2K event samples were evaluated for the joint analysis.

Event selection—This analysis uses a total of eighteen SK atmospheric and five T2K event samples, constructed as described in Refs. [9] and [15]. The event selections are based primarily on the number of reconstructed Cherenkov rings, the type of those rings, and the number of delayed Michel electron candidates. The ring types are either showering (e -like) or non-showering (μ -like) and are the basis of the separation between $\bar{\nu}_e$ and $\bar{\nu}_\mu$ events. The T2K selections target events with little activity in the SK outer detector, so-called fully contained (FC) events, with a single Cherenkov ring. This topology primarily selects charged current quasi-elastic (CCQE)-like events, although in neutrino running mode an additional sample probes ν_e events containing a below-Cherenkov-threshold π^+ by requiring exactly one e -like ring and one Michel electron. Atmospheric neutrinos span a much wider range of energies, and the atmospheric FC sample is divided into sub- and multi-GeV categories based on the deposited visible energy in the detector. The SK analysis additionally includes events with significant energy deposition in the outer detector. The T2K beam samples and FC single-ring sub-GeV atmospheric samples in SK have a large kinematic overlap, but differ slightly in their respective event selections, which remain the same as in the publications above. One additional selection criterion, however, is applied to both the SK FC and T2K samples to remove neutron contamination from the Michel candidates for each event, which changes the event rates by $\mathcal{O}(1\%)$.

Interaction model—Neutrino interactions are simulated with the NEUT generator v5.4.0 [16] using the same configuration as T2K’s analysis [8]. The common “low-energy” uncertainty model used for the T2K and atmospheric SK FC sub-GeV samples is based on T2K’s model, with additions to cover important uncertainties for the SK atmospheric analysis. Additional normalization uncertainties on the neutral current single π^0 model are introduced, which scale the resonant and coherent contributions separately, motivated by studies of Mini-BooNE data [17, 18]. A supplementary uncertainty on the CCQE cross-section ratio $\sigma_{\nu_e}/\sigma_{\nu_\mu}$ is added based on the difference of this ratio between the spectral function model [19] used in this analysis and new calculations using the Hartree-Fock model with Continuum Random Phase Approximation [20, 21]. The ability of the low energy model to describe the atmospheric sub-GeV data

samples is evaluated by comparing its predictions using T2K’s ND constraint to the observed data for the down-going part of those samples. The down-going events are mostly unaffected by oscillations, and can therefore be used to test the model without biasing the oscillation measurement. Good agreement with data is found for the samples targeting events without pions in the final state. For the samples targeting charged current single charged pion ($CC1\pi^+$) events, a significant data excess is seen: 225 events are observed for $160.0 \pm 12.6(\text{stat}) \pm 14.3(\text{syst})$ predicted in the e -like sample, and 84 are observed in the μ -like sample for $52.0 \pm 7.2(\text{stat}) \pm 5.3(\text{syst})$ predicted. The excess is localized at low lepton momentum in the e -like sample, and uniformly distributed in the μ -like sample. An excess is also seen at low momentum in the corresponding e -like beam sample, but is not significant due to the low statistics of this sample. As a result of the observed excesses, an interaction model uncertainty is added to change the shape of the pion three-momentum spectrum for charged-current resonant interactions by modifying the Adler angle [22] distribution, based on theoretically motivated [23, 24] and empirical modifications. A reconstruction uncertainty is also added, as detailed in the next section.

The model for the remaining SK samples (“high-energy model”) is based on that used in the SK analysis, but shares the CCQE part with the low-energy model with the exception of the high Q^2 (four-momentum transfer) parameters, due to similarities in the CCQE events’ phase space outside of the high Q^2 region. SK and T2K’s uncertainty models for resonant production and deep inelastic scattering events are very similar, the main difference being the existence of additional parameters and different nominal values in SK’s analysis. For consistency, the single pion production parameters are set to the same values as in T2K, which come from studies of external data. This increases uncertainties compared to SK’s analysis. The model for pion final-state interactions is tuned to external data [25], as done by T2K.

Data from T2K’s ND are used to constrain uncertainties on the interaction parameters from the low-energy model and the correlated part of the high-energy model, but not on the new uncertainties added for this analysis, or any other aspect of the high-energy model, due to the lack of overlapping phase space between the near-detector and non-sub-GeV atmospheric samples.

Detector model—The same version of the SK event reconstruction algorithm [9] is used for the two experiments, to be able to derive correlations between their detector and reconstruction systematic uncertainties. Many of the detector uncertainties in both SK and T2K’s analyses are estimated from comparisons between atmospheric data and simulation. For these, correlated uncertainties are constructed by evaluating the effects of variations of the detector parameters of the SK model on the number of events in the different samples of the two experiments simultaneously. Correlations between the reconstructed momentum scale uncertainty of the two ex-

periments are found to have an impact on the constraint on Δm_{32}^2 obtained in the data fit. Three of the four analyses described in the next section treat the corresponding parameters as correlated, while the fourth considers them uncorrelated. The remaining detector uncertainties from the reference SK and T2K analyses that are relevant for only one of the experiments are applied to the corresponding samples. An additional systematic uncertainty is introduced for the sub-GeV samples targeting $CC1\pi^+$ events. It allows single ring single Michel electron events with low lepton momentum to migrate between ν_e -like and ν_μ -like samples. The size of this uncertainty covers the excess in data observed for the down-going $CC1\pi^+$ ν_e -like events at low momentum.

Oscillation analysis—Two Bayesian and two frequentist analyses based on the model described above but with differences in technical implementation, binning, and statistical methodology are used to fit the data. To constrain uncertainties using the T2K ND, one analysis performs simultaneous fits of the T2K ND, T2K far detector and SK atmospheric data, while the others use a covariance matrix to encode T2K’s ND constraint on systematic parameters when fitting the events observed at SK. The Bayesian analyses use Markov Chain Monte Carlo methods to evaluate marginal likelihoods for the parameters of interest, while the frequentist analyses compute the profile likelihood on a fixed grid of values of the oscillation parameters of interest. For atmospheric oscillation probability calculations, path-dependent density averaging of the matter effect based on a four layer approximation of the PREM model [26] is used, and the fast atmospheric oscillations at low energy are smeared using different techniques depending on the analysis. The path-dependence yields more precise oscillation probabilities than the conventional approximation assuming layers of constant density. All analyses utilize a binned log-likelihood test statistic assuming Poisson-distributed bin contents plus Gaussian penalties for the systematic parameters. Finally, reactor experiment measurements of θ_{13} using $\bar{\nu}_e$ disappearance, $\sin^2 2\theta_{13} = 0.0853 \pm 0.0027$ [2, 27–30], are used as an external constraint.

Robustness studies—Simulated datasets [8] are used to test the robustness of the analysis to effects not included in the base systematic uncertainty model. They are generated using alternative models, and fitted using the nominal model to measure how the obtained p -values and constraints on oscillation parameters would be affected by having assumed the wrong model. Fourteen such simulated datasets are considered, corresponding to alternative neutrino interaction models and data-driven effects at both T2K ND and SK. These studies are used to estimate, amongst other things, how much the data excess observed in the atmospheric down-going $CC1\pi^+$ samples could bias the results despite the newly added uncertainties if it was coming from an unknown systematic effect. Some of the simulated datasets produce a

visible shift in the preferred values for Δm_{32}^2 . The uncertainty on Δm_{32}^2 is inflated by $3.6 \times 10^{-5} \text{ eV}^2/c^4$ to account for these effects.

Dataset—The atmospheric dataset is slightly increased compared to [9] to include the full Super-Kamiokande IV period (2008–2018), corresponding to a total live-time of 3244.4 days. The same T2K dataset as in [8] is used, corresponding to exposures of 19.7×10^{20} and 16.3×10^{20} protons on target in neutrino and antineutrino running modes, respectively.

Bayesian results—The Bayesian analyses assume uniform priors on δ_{CP} or $\sin \delta_{\text{CP}}$, $\sin^2 \theta_{23}$, Δm_{32}^2 , and the MO. They find a preference for the normal ordering, and a weak preference for the upper octant (Table I). SK and T2K data prefer different octants which leads the joint analysis to have a weaker octant constraint than the individual experiments and a higher probability for maximal mixing, while for the CP-violating phase, both experiments favor similar values (Figure 1). The exclusion of the CP conserving values of J_{CP} (Figure 2) and δ_{CP} is quantified by determining the largest fraction of the posterior density for which the value considered is not included in either of the corresponding highest posterior density credible intervals obtained by the two Bayesian analyses (Table II).

TABLE I. Octant and MO posterior probabilities using either the full dataset or samples from only one experiment and assuming equal prior probabilities. Values obtained by the second analysis are shown in parentheses.

	SK only	T2K only	SK+T2K
Upper octant	0.318 (0.337)	0.785 (0.761)	0.611 (0.639)
Normal ordering	0.654 (0.633)	0.832 (0.822)	0.900 (0.887)

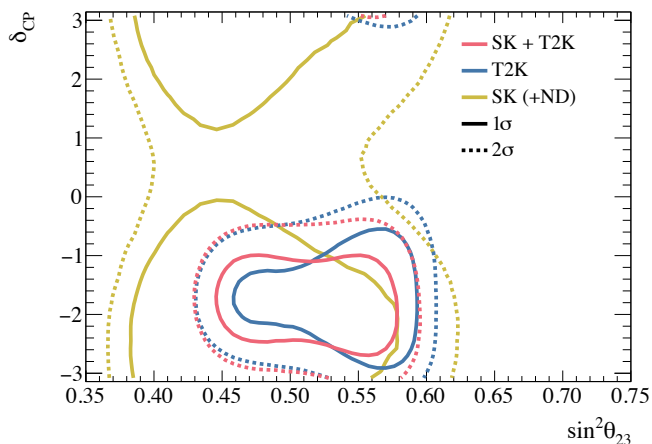


FIG. 1. The $(\sin^2 \theta_{23}, \delta_{\text{CP}})$ credible regions obtained with the SK, T2K, and combined datasets. The MO is marginalized over and a prior uniform in δ_{CP} is used.

Frequentist results—Ensembles of pseudo-experiments are constructed to evaluate the frequentist significance

TABLE II. Largest credible interval from the Bayesian analyses not containing different CP conserving values of J_{CP} and δ_{CP} . Values in parentheses indicate how these could change due to possible biases seen in robustness studies.

Value tested	Prior uniform in	
	δ_{CP}	$\sin(\delta_{\text{CP}})$
$J_{\text{CP}} = 0$	2.3σ (2.2σ)	2.0σ (1.9σ)
$\delta_{\text{CP}} = 0$	2.6σ (2.5σ)	2.3σ (2.2σ)
$\delta_{\text{CP}} = \pi$	2.1σ (1.9σ)	1.6σ (1.4σ)

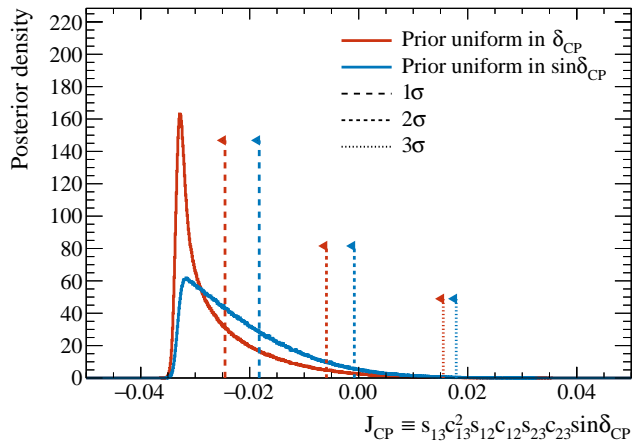


FIG. 2. The posterior density for the Jarlskog invariant with credible intervals overlaid, marginalized over both MOs, and assuming a uniform prior in either δ_{CP} or $\sin \delta_{\text{CP}}$.

of the CP and MO results, taking into account statistical fluctuations and randomizing the values of nuisance oscillation and systematic parameters according to their posterior [31] and prior probability distributions respectively. Estimating the significance of CP conservation (CPC) based on the presence or not of both 0 and π in the δ_{CP} confidence intervals was found to have significant over-coverage. Instead, the log-likelihood ratio between assuming CPC ($\sin \delta_{\text{CP}} = 0$, here equivalent to $J_{\text{CP}} = 0$) and without any assumption is used as a test statistic. For the neutrino MO, the log-likelihood ratio between normal and inverted ordering is used (Figure 3).

The obtained p -values are summarized in Table III. CPC is disfavored with a lower p -value ($p = 0.037$) than when using only the T2K data ($p = 0.047$). Good agreement ($p = 0.75$) is found with an ensemble that allows for CP-violation by assuming posterior-distributed δ_{CP} values. The inverted ordering is disfavored while good agreement with the normal ordering hypothesis is found, resulting in a CL_s parameter [32] for the inverted ordering of 0.18. The distribution of the MO test statistic depends on the assumed values of $\sin^2 \theta_{23}$ (from SK samples) and δ_{CP} (from T2K samples). The p -value for the inverted ordering varies between 0.05 and 0.08 when assuming different fixed true values for $\sin^2 \theta_{23}$ and δ_{CP} over the range of their 90% confidence intervals. The best-fit values and 68.3% confidence intervals obtained

using the Feldman–Cousins method [33] where necessary, are $\delta_{\text{CP}} = -1.76_{-0.95}^{+0.73}$, $\sin^2 \theta_{23} = 0.468_{-0.025}^{+0.106}$, where MO was treated as a nuisance parameter, and Δm_{32}^2 ($|\Delta m_{31}^2|$) = $2.520_{-0.058}^{+0.048}$ ($2.480_{-0.048}^{+0.052}$) $\times 10^{-3}$ eV² for normal (inverted) ordering.

TABLE III. Frequentist p -values for the different CP and MO hypotheses. The most conservative of the two values obtained by the frequentist analyses is given. “ p -studies” corresponds to the value up to which each p -value could increase due to biases seen in robustness studies.

Hypothesis	p -value	p -studies
CP conservation	0.037	0.050
Inverted ordering	0.079	0.080
Normal ordering	0.58	—

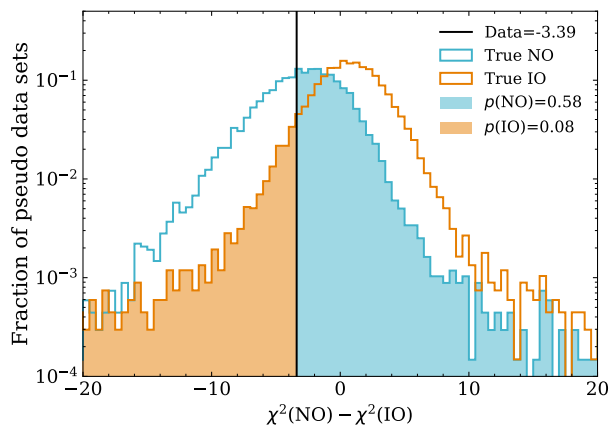


FIG. 3. Distribution of the MO test statistic under true normal and inverted ordering hypotheses. The filled areas to the left (right) of the data result indicate the p -values for the inverted (normal) hypotheses.

Goodness of fit—The Bayesian analyses find good posterior predictive p -values [34] using both the event spectra ($p = 0.24$) and total event counts ($p = 0.19$). The p -values for the individual T2K samples agree with the reference T2K analysis [8] up to small differences coming predominantly from model changes. The frequentist p -values [35] additionally show good consistency between the values of the systematic parameters favored by the T2K ND and atmospheric data ($p = 0.19$), as well as between the atmospheric and beam samples ($p = 0.24$).

Discussion—The SK and T2K datasets favor similar values for the CP phase, close to maximal CP violation, and both show a preference for the normal MO. As a result, the combined analysis finds increased preferences for non-conservation of CP symmetry and the normal ordering. When looking directly at the exclusion of CPC through the presence of $J_{\text{CP}} = 0$ in credible intervals or frequentist p -values, an exclusion at the 2σ level is found. However, the significance can fall below 2σ due to

the potential weaknesses of the uncertainty model tested using simulated datasets. The alternative models having the most impact are the one assuming that the excess seen for down-going CC1 π^+ -like events is fully due to an unknown systematic effect, and an alternative nuclear model for CCQE interactions [36]. This indicates areas where the robustness of the model should be improved for future analyses.

Conclusion—The SK and T2K collaborations have produced a first joint analysis of their data. A common neutrino interaction and detector model has been developed for the events of the two experiments which overlap in energy, and is found to be able to properly describe the two datasets. The results show an exclusion of the CP-conserving value of the Jarlskog invariant with a significance between 1.9σ and 2.0σ , a limited preference for the normal ordering, and no strong preference for the θ_{23} octant. This first joint analysis is also an important step towards the combined beam and atmospheric data analyses planned by next generation neutrino oscillation experiments.

ACKNOWLEDGEMENTS

The Super-Kamiokande collaboration gratefully acknowledges cooperation of the Kamioka Mining and Smelting Company. The Super-Kamiokande experiment was built and has been operated with funding from the Japanese Ministry of Education, Science, Sports and Culture, and the U.S. Department of Energy.

The T2K collaboration would like to thank the J-PARC staff for superb accelerator performance. We thank the CERN NA61/SHINE Collaboration for providing valuable particle production data. We acknowledge the support of MEXT, JSPS KAKENHI and bilateral programs, Japan; NSERC, the NRC, and CFI, Canada; the CEA and CNRS/IN2P3, France; the DFG, Germany; the NKFIH, Hungary; the INFN, Italy; the Ministry of Science and Higher Education (2023/WK/04) and the National Science Centre (UMO-2018/30/E/ST2/00441, UMO-2022/46/E/ST2/00336 and UMO-2021/43/D/ST2/01504), Poland; the RSF (RSF 24-12-00271) and the Ministry of Science and Higher Education, Russia; MICINN and ERDF funds and CERCA program, Spain; the SNSF and SERI, Switzerland; the STFC and UKRI, UK; the DOE, USA; and NAFOSTED (103.99-2023.144), Vietnam. We also thank CERN for the UA1/NOMAD magnet, DESY for the HERA-B magnet mover system, the BC DRI Group, Prairie DRI Group, ACENET, SciNet, and CalculQuebec consortia in the Digital Research Alliance of Canada, GridPP and the Emerald High Performance Computing facility in the United Kingdom, and the CNRS/IN2P3 Computing Center in France. In addition, the participation of individual researchers and institutions has been further supported by funds from the ERC (FP7), “la Caixa” Foundation, the Eu-

European Union's Horizon 2020 Research and Innovation Programme under the Marie Skłodowska-Curie grant; the JSPS, Japan; the Royal Society, UK; French ANR and Sorbonne Université Emergences programmes; the VAST-JSPS (No. QTJP01.02/20-22); and the DOE

Early Career programme, USA. For the purposes of open access, the authors have applied a Creative Commons Attribution license to any Author Accepted Manuscript version arising.

-
- [1] Y. Fukuda *et al.* (Super-Kamiokande Collaboration), Evidence for oscillation of atmospheric neutrinos, *Phys. Rev. Lett.* **81**, 1562 (1998).
- [2] M. Tanabashi *et al.* (Particle Data Group), Review of particle physics, *Phys. Rev. D* **98**, 030001 (2018), and 2019 update.
- [3] C. Jarlskog, Commutator of the quark mass matrices in the standard electroweak model and a measure of maximal CP nonconservation, *Phys. Rev. Lett.* **55**, 1039 (1985).
- [4] C. Jarlskog, Invariants of lepton mass matrices and cp and t violation in neutrino oscillations, *Physics Letters B* **609**, 323 (2005).
- [5] Y. Fukuda *et al.* (Super-Kamiokande Collaboration), The Super-Kamiokande detector, *Nucl. Instrum. Meth. A* **501**, 418 (2003).
- [6] K. Abe *et al.* (T2K Collaboration), The T2K Experiment, *Nucl. Instrum. Meth. A* **659**, 106 (2011), arXiv:1106.1238 [physics.ins-det].
- [7] K. Abe *et al.* (T2K Collaboration), Neutrino oscillation physics potential of the T2K experiment, *PTEP* **2015**, 043C01 (2015).
- [8] K. Abe *et al.* (T2K Collaboration), Measurements of neutrino oscillation parameters from the T2K experiment using 3.6×10^{21} protons on target, *Eur. Phys. J. C* **83**, 782 (2023), arXiv:2303.03222 [hep-ex].
- [9] M. Jiang *et al.* (Super-Kamiokande Collaboration), Atmospheric Neutrino Oscillation Analysis with Improved Event Reconstruction in Super-Kamiokande IV, *PTEP* **2019**, 053F01 (2019), arXiv:1901.03230 [hep-ex].
- [10] K. Abe *et al.* (T2K Collaboration), T2K neutrino flux prediction, *Phys. Rev. D* **87**, 012001 (2013).
- [11] M. Honda, T. Kajita, K. Kasahara, and S. Midorikawa, Improvement of low energy atmospheric neutrino flux calculation using the jam nuclear interaction model, *Phys. Rev. D* **83**, 123001 (2011).
- [12] S. Haino *et al.*, Measurements of primary and atmospheric cosmic-ray spectra with the bess-tev spectrometer, *Physics Letters B* **594**, 35 (2004).
- [13] K. Abe *et al.*, Measurements of proton, helium and muon spectra at small atmospheric depths with the bess spectrometer, *Physics Letters B* **564**, 8 (2003).
- [14] N. Abgrall *et al.* (NA61/SHINE), Measurements of π^\pm differential yields from the surface of the T2K replica target for incoming 31 GeV/c protons with the NA61/SHINE spectrometer at the CERN SPS, *Eur. Phys. J. C* **76**, 617 (2016), arXiv:1603.06774 [hep-ex].
- [15] K. Abe *et al.* (T2K Collaboration), Improved constraints on neutrino mixing from the T2K experiment with 3.13×10^{21} protons on target, *Phys. Rev. D* **103**, 112008 (2021), arXiv:2101.03779 [hep-ex].
- [16] Y. Hayato and L. Pickering, The NEUT neutrino interaction simulation program library, *Eur. Phys. J. ST* **230**, 4469 (2021), arXiv:2106.15809 [hep-ph].
- [17] A. A. Aguilar-Arevalo *et al.* (MiniBooNE), Measurement of ν_μ and $\bar{\nu}_\mu$ induced neutral current single π^0 production cross sections on mineral oil at $E_\nu \sim \mathcal{O}(1\text{GeV})$, *Phys. Rev. D* **81**, 013005 (2010), arXiv:0911.2063 [hep-ex].
- [18] P. Stowell *et al.*, NUISANCE: a neutrino cross-section generator tuning and comparison framework, *JINST* **12** (01), P01016, arXiv:1612.07393 [hep-ex].
- [19] O. Benhar, A. Fabrocini, S. Fantoni, and I. Sick, Spectral function of finite nuclei and scattering of GeV electrons, *Nucl. Phys.* **A579**, 493 (1994).
- [20] A. Nikolakopoulos, M. Martini, M. Ericson, N. Van Dessel, R. González-Jiménez, and N. Jachowicz, Mean-field approach to reconstructed neutrino energy distributions in accelerator-based experiments, *Phys. Rev. C* **98**, 054603 (2018).
- [21] A. Nikolakopoulos, N. Jachowicz, N. Van Dessel, K. Niewczas, R. González-Jiménez, J. M. Udías, and V. Pandey, Electron versus muon neutrino induced cross sections in charged current quasielastic processes, *Phys. Rev. Lett.* **123**, 052501 (2019).
- [22] S. L. Adler, Photo-, electro-, and weak single-pion production in the (3,3) resonance region, *Annals of Physics* **50**, 189 (1968).
- [23] D. Rein and L. M. Sehgal, Neutrino Excitation of Baryon Resonances and Single Pion Production, *Annals Phys.* **133**, 79 (1981).
- [24] R. P. Feynman, M. Kislinger, and F. Ravndal, Current matrix elements from a relativistic quark model, *Phys. Rev. D* **3**, 2706 (1971).
- [25] E. S. P. Guerra *et al.*, Using world π^\pm -nucleus scattering data to constrain an intranuclear cascade model, *Phys. Rev. D* **99**, 052007 (2019).
- [26] A. M. Dziewonski and D. L. Anderson, Preliminary reference earth model, *Physics of the Earth and Planetary Interiors* **25**, 297 (1981).
- [27] F. P. An *et al.* (Daya Bay Collaboration), New measurement of θ_{13} via neutron capture on hydrogen at daya bay, *Phys. Rev. D* **93**, 072011 (2016).
- [28] F. P. An *et al.* (Daya Bay Collaboration), Measurement of electron antineutrino oscillation based on 1230 days of operation of the daya bay experiment, *Phys. Rev. D* **95**, 072006 (2017).
- [29] Y. Abe *et al.* (Double CHOOZ Collaboration), Measurement of θ_{13} in double chooz using neutron captures on hydrogen with novel background rejection techniques, *Journal of High Energy Physics* **2016**, [https://doi.org/10.1007/JHEP01\(2016\)163](https://doi.org/10.1007/JHEP01(2016)163) (2016).
- [30] J. H. Choi *et al.* (RENO Collaboration), Observation of energy and baseline dependent reactor antineutrino disappearance in the reno experiment, *Phys. Rev. Lett.* **116**, 211801 (2016).
- [31] R. D. Cousins and V. L. Highland, Incorporating systematic uncertainties into an upper limit, *Nucl. Instrum. Meth. A* **320**, 331 (1992).

- [32] A. L. Read, Presentation of search results: the cls technique, *Journal of Physics G: Nuclear and Particle Physics* **28**, 2693 (2002).
- [33] G. Feldman and R. Cousins, A unified approach to the classical statistical analysis of small signals, *Phys.Rev.D* **57**:3873-3889 (1998).
- [34] A. Gelman, X.-L. Meng, and H. Stern, Posterior predictive assessment of model fitness via realized discrepancies, *Statistica Sinica* **6**, 733 (1996).
- [35] M. Maltoni and T. Schwetz, Testing the statistical compatibility of independent data sets, *Phys. Rev. D* **68**, 033020 (2003), arXiv:hep-ph/0304176.
- [36] J. Nieves, I. R. Simo, and M. J. V. Vacas, Inclusive charged-current neutrino-nucleus reactions, *Phys. Rev. C* **83**, 045501 (2011).